Transition from Solution to the Solid State in Polymer Solar Cells Cast from Mixed Solvents

Jeffrey Peet,[†] Nam Sung Cho,[‡] Sang Kyu Lee,[‡] and Guillermo C. Bazan*[,†,‡]

Department of Materials and Department of Chemistry & Biochemistry, University of California, Santa Barbara, California 93106

Received August 27, 2008; Revised Manuscript Received September 17, 2008

ABSTRACT: Certain solvent additives significantly affect the morphology of the active layer in bulk heterojunction (BHJ) conjugated polymer solar cells and improve the device performance. Previous examinations of the BHJ films have shown that the best additives are characterized by higher boiling points than the host solvent and are poorer solvents for the conjugated host polymer than for the fullerene acceptor; however, little in the way of a mechanistic explanation has been presented, particularly on the dynamics of the transition from solution to the bulk material. This article combines spectroscopic analysis in various solvent mixtures and during solvent evaporation to show that a key feature of the film growth concerns aggregation of polymer chains into more ordered supramolecular structures prior to complete drying. The driving force for aggregation occurs in a medium that (a) is more fluid and allows chains to find optimal registry or conformations and (b) can solvate the fullerenes. We propose that when a single solvent that is good for the two components of the BHJ blend is used, the chains remain solvated up to a point where viscosity inhibits their motion and they are unable to attain similar packing characteristics.

Introduction

Advances in synthetic organic chemistry have given rise to an extraordinary diversity of accessible structures and properties within the realm of organic semiconducting materials.[1,2] There remain, however, poorly understood phenomena at the intersection between synthetic chemistry, which predominantly concerns isolated molecules, and solid state optoelectronic properties, which are often affected as much by mesoscale and macroscale phenomena as by the molecular composition of the components.[3] Unlike highly ordered crystalline inorganic semiconductors, whose properties can be anticipated with excellent precision, the electronic properties of disordered organic systems are difficult to predict due to their extraordinary dependence on processing history.[4−6] The complex relationships between molecular connectivity, processing methodology, and solid state electronic properties have resulted in a great deal of frustration throughout the development of organic optoelectronic materials and devices.

Quintessential examples of how processing conditions, interfacial effects, adsorption properties, and thermal history influence the electronic properties of *single* component films can be found in systems comprising even the most structurally basic polymers and small molecules. Early work with poly(acetylene), the simplest conjugated polymer, yielded enormous variations in conductivity depending on the precise synthetic approach, doping technique, or characterization method.[7,8] Pentacene thin film transistors (TFTs) similarly yield a wide range of properties depending on device geometry, evaporation rate, substrate temperature, and thermal processing history.[9,10] High-performance solution-processable single component TFT polymers, such as poly(2,5-bis(3-dodecylthiophen-2-yl)thieno[3,2-*b*]thiophene) (pBTTT), show complex phase behavior and charge carrier mobilities that depend on thermal history and other processing parameters.[11]

Conjugated polymer-based solar cells based on bulk heterojunction (BHJ) materials provide an even higher order level of complexity, relative to single component devices.[12,13] However, they afford some of the highest power conversion efficiencies (PCE for solution-processed photovoltaic) devices and are thus of great scientific interest and technological importance.[14−16] The BHJ approach requires interpenetrating domains of donor and acceptor phases of specific dimensions and structure throughout the active layer of the device.[17] Furthermore, the internal order within each phase, and specifically the interchromophore distance/orientation, is important to optimize and balance mobilities of electrons within the acceptor domains and holes within the donor domains.[18] It would be ideal from a practical perspective if these interpenetrating structures self-assembled into the optimal arrangement as the system evolves from an isotropic solution into the solid state.

We recently reported that a substantial improvement in the PCE of polymer solar cells is achieved via the incorporation of a small percentage of specific additives into solvents from which BHJ layers are cast.[14] Initial observations were made on blends of poly(3-hexylthiophene) (P3HT) and [6,6]-phenyl C_{61}-butyric acid methyl ester (C_{61}-PCBM) cast from solutions containing a small percentage of alkylthiol additives.[19−21] Steady state and transient photoconductivity revealed an order of magnitude increase in the photoresponsivity of the films processed with additives when compared to films spun from pristine solvent. Increases in hole mobility were consistent with enhanced structural order inferred from X-ray diffraction and optical absorption measurements. The additive approach also proved useful with an amorphous low-bandgap polymer; the PCE of BHJ solar cells was significantly increased without greatly altering the film thickness, the optical density, or the charge carrier mobility of the active layer by incorporating a few volume percent of 1,8-octanedithiol (ODT) into the solvent used to cast the active layer. The blends in that study comprised C_{71}-PCBM as the acceptor and poly[2,6-(4,4-bis(2-ethylhexyl)-4*H*-cyclopenta[2,1-*b*;3,4-*b*′]dithiophene)-*alt*-4,7-(2,1,3-benzothiadiazole)] (PCPDTBT, illustrated in Figure 1) as the electron donor. Of significance is that the PCE was on the order of 5.5%. Subsequent examination of already formed PCPDTBT/C_{71}-PCBM BHJ films using atomic force microscopy (AFM) and transmission electron microscopy (TEM) yielded two criteria

* Corresponding author. E-mail: Bazan@chem.ucsb.edu.
[†] Department of Materials.
[‡] Department of Chemistry and Biochemistry.

10.1021/ma801945h CCC: $40.75
Published on Web 10/28/2008

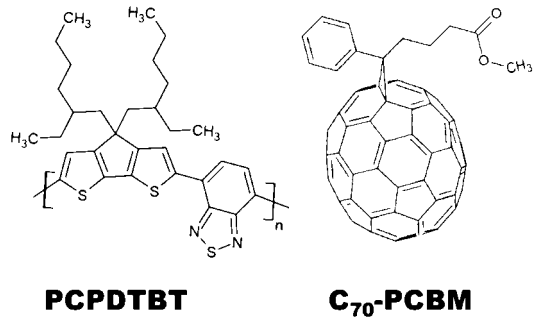

Figure 1. Molecular structures of PCPDTBT (donor) and C_{71}-PCBM (acceptor).

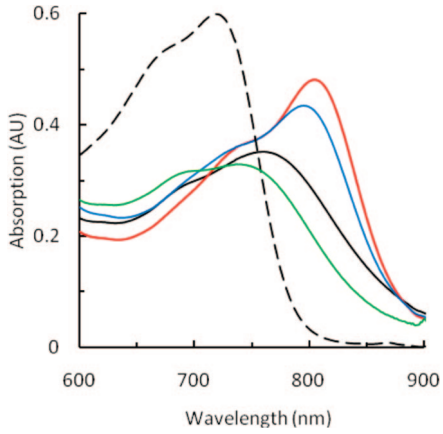

Figure 2. Absorption spectra of PCPDTBT:C_{71}-PCBM mixtures in CB solution (dotted line) and as films cast from CB before (black) and after thermal annealing (green), and cast from CB with 2% ODT (blue), and CB with 2% DIO (red).

for selecting additives: (i) the donor and acceptor must have differential solubility in the additive, and (ii) the additive must have a higher boiling point than the host solvent.[20,22]

In this contribution we examine how additives influence the PCPDTBT and C_{71}-PCBM organization in solution *prior to* and *during* film formation. Such studies give insight into the dynamics of ordering and are differentiated from previous work that focused on examination of solid state structural features and optimization of solar cell devices.[22] A drying process is identified in which the transition from good to poor solvent causes stronger interchain registry and a concomitant red shift in the absorption. Furthermore, we find that the molecular weight of PCPDTBT is critical for attaining the desired morphology; this observation may account for the influence of batch-to-batch variations on solar cell performance.

Results

Optical Characterization of Films. Figure 2 shows the absorption spectra of a 1:3 (w:w) blend of PCPDTBT and C_{71}-PCBM in solution and as a film cast from chlorobenzene (CB) and CB with ODT or 1,8-diiodooctane (DIO). Both ODT and DIO have been shown to be useful additives and are better solvents for C_{71}-PCBM than for PCPDTBT.[22] The specific blend composition ratio was chosen as the test case in all our studies because it has been used as the active layer in some of the highest performance solar cells observed and has been previously shown to be sensitive to additive processing. For example, the PCE increases from 3% to 5.5% upon addition of 2% ODT to the CB host solvent.[14] The films in Figure 2 were cast on quartz substrates at 1200 rpm from solutions containing 10 mg/mL of PCPDTBT and 30 mg/mL of C_{71}-PCBM. Film thicknesses were ~100 nm, as determined by scratching the film and measuring the trench depth by AFM. As shown in Figure 2, there is a shift in the absorption maxima from 715 nm in solution to 760 nm in the films cast from pure CB. This red shift indicates a significant amount of either interchain delocalization or chain planarization as the polymer transitions into the solid state.[23,24] Additionally, films cast from CB with either 2% ODT or 2% DIO are further red-shifted, to 795 and 800 nm, respectively, but a film thermally annealed at 150 °C for 15 min is blue-shifted to 736 nm. The peak near 800 nm is characteristic of films that yield high-efficiency solar cells.[14]

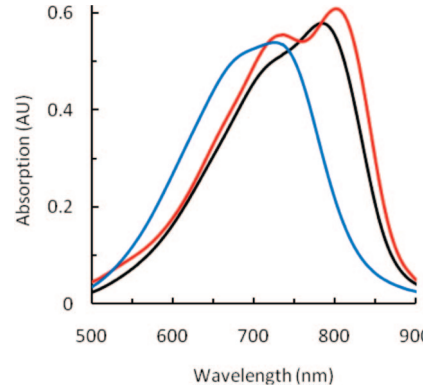

Figure 3. Absorption of PCPDTBT films cast from CB (black) compared with CB containing 2% DIO as cast (red) and after thermal annealing at 150 °C (blue).

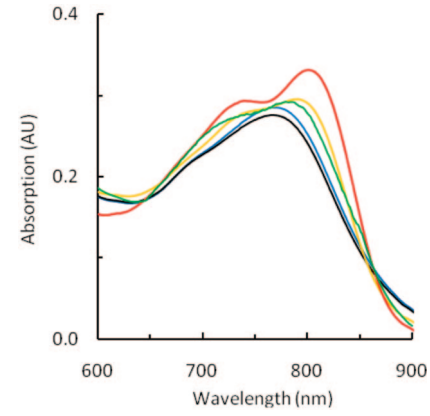

Figure 4. Normalized absorption of PCPDTBT/C_{71}-PCBM films cast from TCB (black, bp = 214 °C) at 1200 rpm and cast from TCB with 2% of OT (blue, bp = 200 °C), ODT (orange, bp = 270 °C), and diiodooctane (red, bp = 327 °C). The absorption of a film cast from CB (bp = 131 °C) with 2% *n*-octanethiol is normalized at 600 nm and shown in green for comparison.

Films containing only the PCPDTBT component were examined as a function of solvent composition and thermal history. Comparison of the absorption maximum of a PCPDTBT film obtained from CB (780 nm), shown in black in Figure 3, against that of PCPDTBT:C_{71}-PCBM (760 nm) presented in Figure 2, indicates that the formation of the low energy component is frustrated by the presence of C_{71}-PCBM. Addition of 2% DIO to the solvent used to cast the PCPDTBT film increases the vibronic definition and further red-shifts the absorption to 785 nm (red curve in Figure 3). Heating the films at 150 °C for 15 min under nitrogen results in a blue shift in the absorption to 735 nm.

To determine if the effect of the additives is primarily due to a decrease in the evaporation rate of the solvent mixture, a series of PCPDTBT/C_{71}-PCBM films were cast from 1,2,4-trichlorobenzene (TCB) as the primary solvent, as shown in Figure 4. TCB has a boiling point of 214 °C and is thus expected to evaporate more slowly than CB (bp = 131 °C). The data in

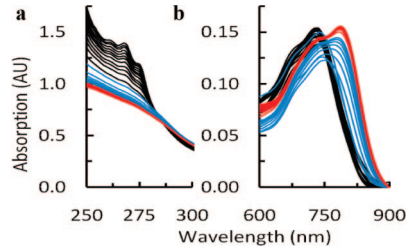

Figure 5. Absorption spectra in the (a) 250−300 nm range and (b) 600−900 nm range as a function of time after spin-coating for 10 s at 2000 rpm from TCB with 2% DIO in 90 s intervals (black and blue) and then 10 min intervals (red).

Figure 4 show that the absorption maxima of films cast from TCB (768 nm) are only slightly red-shifted relative to the maxima of films cast from CB (760 nm). In previous studies *n*-octanethiol (OT, bp = 199 °C) was effectively used as a solvent additive with P3HT-based BHJ solar cells using CB as the primary solvent.[21] As shown in Figure 4, OT red shifts the absorption peak of a PCPDTBT:C_{71}-PCBM blend film from 760 to 786 nm when used as an additive in CB; however, when used as an additive in TCB there is no red shift (peak maximum at 767 nm). When ODT (bp = 270 °C) or DIO (bp = 327 °C) is used as additive in TCB, the absorption red shifts to 790 or 800 nm, respectively. This collected set of observations confirms that neither an additive with a boiling point below that of the primary solvent nor a slow drying solvent is sufficient to red shift the PCPDTBT absorption in these BHJ films; it is critical that the solvent additive must have a boiling point above that of the primary solvent.

A series of measurements were designed to probe changes in absorption as the solvent evaporates and the blend transitions from a solvated system to a solid film.[25] These experiments begin by casting PCPDTBT:C_{71}-PCBM from TCB with 2% DIO onto quartz and spinning (2000 rpm) for a short time (10 s) so that solvent evaporation is incomplete. The substrate is then monitored inside a spectrometer which is not sealed between measurements, and thus solvent vapor is allowed to escape. Figure 5 shows the resulting absorption spectra as a function of time. Two regions of the spectrum are highlighted: 250−300 and 600−900 nm. As described previously, the latter portion corresponds to the changes in PCPDTBT absorption. Both TCB and DIO absorb near 250 nm; however, the TCB absorption shows vibronic structure, whereas the DIO absorption does not. This difference can be used to determine the point at which the TCB is largely depleted. As shown in Figure 5, the vibronic structure is maintained for ∼18 min. At the point where the remnants of vibronic structure disappear, shown in Figure 5 by the change in curve colors from black to blue, the PCPDTBT absorption begins to shift to longer wavelengths and reaches a steady state ∼28 min after casting. The absorption at 250 nm continues to slowly decrease for several hours afterward, as shown by the spectra shown in red (after the drying process is complete, the additives are no longer detectable in the film by X-ray photoelectron spectroscopy or infrared spectroscopy).[14,25] We can thus conclude that the polymer absorption red shift occurs prior to the complete removal of volatiles; what appears to be the final state of the polymer is reached while the film is still wet with additive. These observations, coupled with the fact that the degree of delocalization is greater in the additive-processed film, indicate that solvation during the liquid to solid transition influences either the solid state packing or the conformation of the polymer chains.

Optical Characterization in Solution. Poor solvation effects induced by the additive were examined by dissolving a PCPDTBT/C_{71}−PCBM blend into CB/DIO mixtures ranging

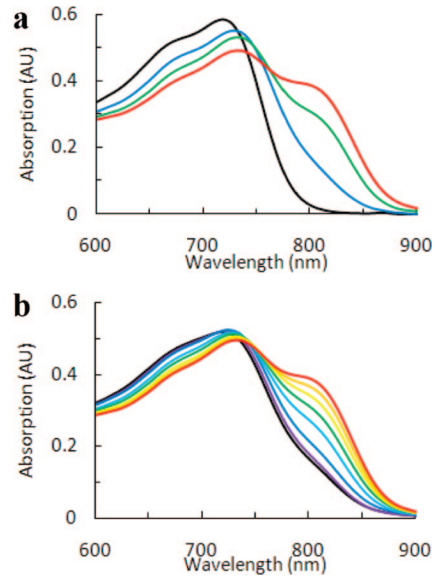

Figure 6. (a) Absorption of a 1:3 blend of PCPDTBT:C_{71}-PCBM dissolved in CB:DIO ratios of 1:0 (black), 1:2 (blue), 1:5 (green), and 1:25 (red). (b) Absorption of PCPDTBT:C_{71}-PCBM dissolved in a 1:25 CB:DIO mixture at 80 °C (black), 70 °C (purple), 60 °C (dark blue), 50 °C (light blue), 40 °C (green), 30 °C (yellow), 20 °C (orange), and 15 °C (red). These measurements were made through a 1 mm quartz cuvette.

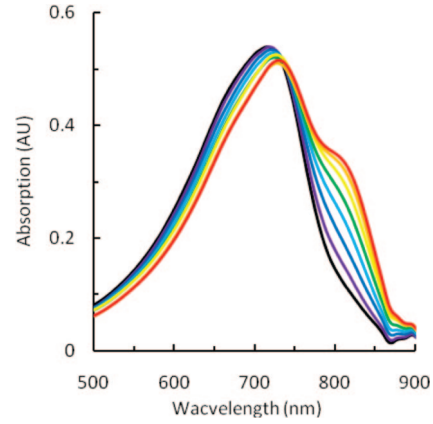

Figure 7. Absorption of PCPDTBT dissolved in pure DIO at 80 °C (black), 70 °C (purple), 60 °C (dark blue), 50 °C (light blue), 40 °C (green), 30 °C (yellow), 20 °C (orange), and 15 °C (red).

from pure CB to 1:25 (v:v) CB:DIO. Absorption measurements were taken at a concentration of 0.07 mg/mL of PCPDTBT and 0.21 mg/mL of fullerene. These relatively dilute conditions were required to prevent PCPDTBT precipitation. As shown in Figure 6A, there is a progressive increase in the contribution by the 800 nm band with increasing DIO content. Figure 6B contains the temperature dependence of the absorption band at 800 nm for the blend in the 25:1 DIO:CB solvent mixture. The contribution from the 800 nm band is reduced with increased temperature and returns when the temperature is lowered. DIO is thus a poor solvent that favors aggregation of PCPDTBT into supramolecular structures in which there is more delocalization. These features are translated into the solid state as shown in Figure 2.

DIO more readily dissolves C_{71}-PCBM than PCPDTBT. However, as shown in Figure 7, it is possible to dissolve sufficient PCPDTBT in DIO (0.005 mg/mL) to record absorption spectra. Significantly, the spectrum at room temperature displays the low-energy band at ∼800 nm. Furthermore, the contribution from this band disappears upon heating the sample (also shown

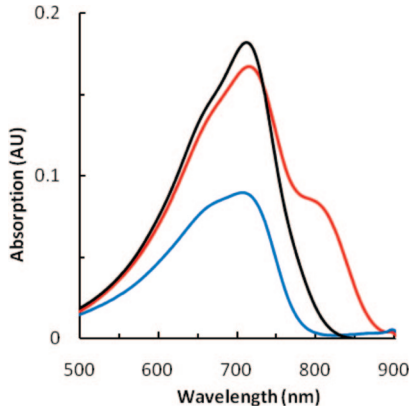

Figure 8. Absorption of PCPDTBT solution in CB (black), in DIO (red), and in DIO after filtration through a 450 nm PTFE filter (blue).

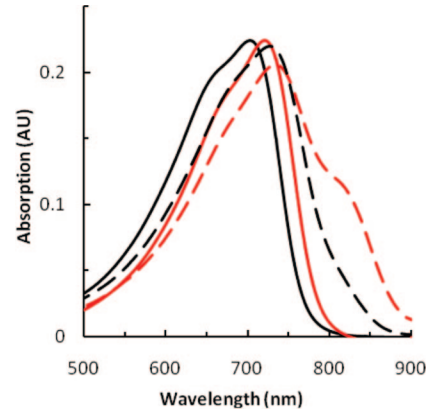

Figure 9. Absorption of PCPDTBT solution in CB solution (solid lines) and in DIO (dashed lines) with $M_n = 7400$ (black) and $M_n = 18\,500$ (red).

in Figure 7). This shift in the absorption spectrum with temperature was observed to be repeatable over multiple temperature cycles. Since the data in the variable temperature and solvent ratio experiments are not normalized and there is no obvious scattering or drop in total optical density, the polymer does not precipitate from solution. The integrated optical density in the 500−900 nm region increases slightly upon aggregation, which is analogous to changes observed in the optical density of P3HT upon crystallization.[19] It should be noted that these solutions are too dilute to cast device quality films; however, they provide insight into the effect of the solvation environment on the interactions of the polymer chains. The changes in optical features presented in Figures 6 and 7 further confirm that the absorption band at 800 nm is due to an aggregate with a higher degree of internal order, which only occurs in a poor solvent.

A final simple test was designed to conclusively identify the species responsible for the band at 800 nm as interchain aggregates.[26] The absorption spectra of PCPDTBT in DIO and in CB at ~0.0025 mg/mL are shown in Figure 8 as the black and blue curves, respectively. If the PCPDTBT solution in DIO is filtered with a 0.45 μm syringe filter, the 800 nm absorption is not observed (blue curve) and the absorption peak drops by 60%. The fact that the 800 nm peak is removed by filtration is an unambiguous indication that this band arises from large multichain species.

Batch to batch variations in PCPDTBT can have a strong influence on solar cell performance.[22] The aggregation of two PCPDTBT samples with different molecular weight characteristics was therefore examined in DIO. One of the batches used for these experiments had a number-average molecular weight (M_n) of 18 500 and a polydispersity index (PDI) of 2. A separate batch was prepared with a $M_n = 7400$ and PDI = 2. The first batch was used as received from Konarka Technologies.[27,28] The second batch was synthesized in our laboratories as described in the literature.[29,30] As shown in Figure 9, while the absorption spectra of the two batches in a good solvent (CB) are similar, only the higher molecular weight batch gives rise to the aggregate band when dissolved in a poor solvent (DIO). Both polymers were dissolved at ~0.0025 mg/mL, and the absorption was measured through a 1 cm path length quartz cuvette. The data indicate a strong dependence of aggregation on the molecular weight of PCPDTBT, as previously observed with other conjugated polymer systems.[31]

Discussion and Conclusion

Solvent additives have been previously shown to improve the function of conjugated polymer solar cells.[14,19] Correlation of the BHJ morphology obtained by AFM and TEM to device performance provided criteria for selection of these additives, namely differential solubility and a higher boiling point than the host solvent.[22] The work presented here focused on the solution characteristics and can be used to build a picture for how the PCPDTBT:C_{71}-PCBM films evolve during evaporation of the solvent. The initial conditions consist of well-solvated chains and fullerene in a solvent mixture that predominantly contains a good host solvent for both species. A wet layer is obtained immediately after spin-casting in which the good solvent begins to evaporate more quickly from the incipient film. As the solvent quality of the matrix begins to deteriorate, from the point of view of PCPDTBT, there is a critical point where the PCPDTBT chains come together and yield aggregates characterized by absorption at higher wavenumbers (800 nm). Whether the red shift in absorption is due to better interchain registry, leading to more efficient interchain delocalization, or a planarization of the polymer backbone conformation remains poorly understood at this juncture. Despite these uncertainties, it is apparent that it is not possible to obtain polymer domains with similar optical/electronic features by slow evaporation of a good solvent or by thermal annealing. Our current thinking is that with the additives the driving force for aggregation occurs in a medium that is more fluid and allows the chains to find optimal registry or conformations. When only a good solvent is present, the chains remain well solvated up to the point where the viscosity of the medium prevents them from being mobile. Also significant is that heating PCPDTBT or PCPDTBT:C_{71}-PCBM films leads to a blue shift in absorption; this suggests that the type of aggregation obtained with the additives may not be thermodynamically favored at elevated temperatures. The critical importance of the solvation environment during the kinetically constrained spin-casting process is thus apparent.

A discussion of the effects of processing additives on PCPDTBT would be incomplete without presenting a number of the significant differences between the effects observed when using P3HT as the donor polymer. Foremost, PCPDTBT:C_{71}-PCBM films obtained from the solvents used in these studies are largely amorphous, as determined by X-ray diffraction. Unlike PCPDTBT films cast from good solvents, P3HT films without fullerene are crystalline independent of additive processing, thermal annealing, or solvent selection; the additive processing only significantly enhances crystallinity in the presence of the fullerene.[32] With the P3HT:C_{61}-PCBM system, the additive processing allows the polymer to more completely crystallize by providing increased drying time during the kinetically limited spin-coating process.[21,33] There are a number of processing techniques in the literature which similarly increase the capacity of P3HT to crystallize.[16,33,34] As discussed above, thermal annealing is not a viable option for optimizing

PCPDTBT-based BHJ films. Furthermore, Figure 4 indicates that slowing evaporation is not effective at increasing PCPDTBT delocalization. The use of additives provides the only known pathway for optimizing PCPDTBT aggregation in BHJ films.

Experimental Section

PCPDTBT with M_n of 18 400 was used as received from Konarka Technologies.[27,28] The synthesis, purification, and fractionation of this material have been previously published. PCPDTBT with M_n of 7400 was synthesized by a similar method.[29,30] C_{71}-PCBM was used as received from Nano-C Inc., and all solvents and additives were used as received from Sigma-Aldrich Inc.

Absorption measurements were measured on quartz substrates using a Shimadzu 2401 diode array spectrometer equipped with a computer-controlled Peltier heating and cooling cuvette holder. Solution absorption studies were conducted in 1 cm quartz cuvettes. Filters used to study polymer aggregation were 0.45 μm Pall PVDF filters.

The film in Figure 5 was scanned every ~90 s (black and blue lines) and then every 10 min (red lines). On the basis of films cast in this manner and films cast from the identical solutions at 1200 RPM for 3 min, there is little effect on the film absorption characteristics resulting from the change in spin-coating conditions that are used for these measurements. Trichlorobenzene was used instead of chlorobenzene to slow the primary solvent evaporation to allow for increased temporal resolution of the drying process. The data in Figure 6 were obtained by dilution of a CB solution containing 10 mg/mL of PCPDTBT and 30 mg/mL of C_{71}-PCBM with mixtures of CB and DIO to obtain a concentration of 0.04 mg/mL of PCPDTBT.

Acknowledgment. The authors acknowledge the DOE, ICB, and ONR for funding, Dr. Dan Moses and Professor Alan Heeger for valuable discussions, and Konarka Technology for providing the PCPDTBT material for study. N.S.C thanks the Korean government KRF-2006-C00064, and J.P. thanks the NDSEG fellowship for support.

References and Notes

(1) Tour, J. M. *Chem. Rev.* **1996**, *96*, 537–553.
(2) Shirota, Y. *J. Mater. Chem.* **2000**, *10*, 1–25.
(3) Bazan, G. C. *J. Org. Chem.* **2007**, *72*, 8615–8635.
(4) Nguyen, T. Q.; Martini, I. B.; Liu, J.; Schwartz, B. J. *J. Phys. Chem. B* **2000**, *104*, 237–255.
(5) Shaheen, S. E.; Brabec, C. J.; Sariciftci, N. S.; Padinger, F.; Fromherz, T.; Hummelen, J. C. *Appl. Phys. Lett.* **2001**, *78*, 841–843.
(6) Blouin, N.; Michaud, A.; Gendron, D.; Wakim, S.; Blair, E.; Neagu-Plesu, R.; Belletete, M.; Durocher, G.; Tao, Y.; Leclerc, M. *J. Am. Chem. Soc.* **2008**, *130*, 732–742.
(7) Fincher, C. R.; Ozaki, M.; Tanaka, M.; Peebles, D.; Lauchlan, L.; Heeger, A. J. *Phys. Rev. B* **1979**, *20*, 1589–1602.
(8) Naarmann, H.; Theophilou, N. *Synth. Met.* **1987**, *22*, 1–8.
(9) Dimitrakopoulos, C. D.; Malenfant, P. R. L. *Adv. Mater.* **2002**, *14*, 99–117.
(10) Gundlach, D. J.; Lin, Y. Y.; Jackson, T. N.; Nelson, S. F.; Schlom, D. G. *IEEE Electron Device Lett.* **1997**, *18*, 87–89.
(11) Kline, R. J.; DeLongchamp, D. M.; Fischer, D. A.; Lin, E. K.; Richter, L. J.; Chabinyc, M. L.; Toney, M. F.; Heeney, M.; McCulloch, I. *Macromolecules* **2007**, *40*, 7960–7965.
(12) Thompson, B. C.; Frechet, J. M. J. *Angew. Chem., Int. Ed.* **2008**, *47*, 58–77.
(13) Coakley, K. M.; McGehee, M. D. *Chem. Mater.* **2004**, *16*, 4533–4542.
(14) Peet, J.; Kim, J. Y.; Coates, N. E.; Ma, W. L.; Moses, D.; Heeger, A. J.; Bazan, G. C. *Nat. Mater.* **2007**, *6*, 497–500.
(15) Kim, J. Y.; Lee, K.; Coates, N. E.; Moses, D.; Nguyen, T. Q.; Dante, M.; Heeger, A. J. *Science* **2007**, *317*, 222–225.
(16) Li, G.; Shrotriya, J. S.; Yao, Y.; Moriarty, T.; Emery, T.; Yang, Y. *Nat. Mater.* **2005**, *4*, 864–868.
(17) Yu, G.; Gao, J.; Hummelen, J. C.; Wudl, F.; Heeger, A. J. *Science* **1995**, *270*, 1789–1791.
(18) Cho, S.; Yuen, J.; Kim, J. Y.; Lee, K.; Heeger, A. J. *Appl. Phys. Lett.* **2007**, *90*, 063511.
(19) Peet, J.; Soci, C.; Coffin, R. C.; Nguyen, T. Q.; Mikhailovsky, A.; Moses, D.; Bazan, G. C. *Appl. Phys. Lett.* **2006**, *89*, 252105.
(20) Yao, Y.; Hou, J.; Xu, Z.; Li, G.; Yang, Y. *Adv. Mater.* **2008**, *18*, 1–7.
(21) Pivrikas, A.; Stadler, P.; Neugebauer, H.; Sariciftci, N. S. *Org. Electron.* **2008**, 000. doi, 10.1016/j.orgel.2008.05.021.
(22) Lee, J. K.; Ma, W. L.; Brabec, C. J.; Yuen, J.; Moon, J. S.; Kim, J. Y.; Lee, K.; Bazan, G. C.; Heeger, A. J. *J. Am. Chem. Soc.* **2008**, *130*, 3619–3623.
(23) Nguyen, T. Q.; Doan, V.; Schwartz, B. J. *J. Chem. Phys.* **1999**, *111*, 4068–4078.
(24) Ariu, M.; Sima, M.; Hill, J.; Fox, A. M.; Lidzey, D. G.; Oda, M.; Cabanillas-Gonzalez, J.; Bradley, D. D. C. *Phys Rev. B* **2003**, *67*, 195333.
(25) Peet, J.; Brocker, E.; Xu, Y. H.; Bazan, G. C. *Adv. Mater.* **2008**, *20*, 1882–1885.
(26) Wu, M.; Kaur, P.; Yue, H.; Clemmens, A. M.; Waldeck, D. H.; Xue, C.; Liu, H. *J. Phys. Chem. B* **2008**, *112*, 3300–3310.
(27) Zhu, Z.; Waller, D.; Gaudiana, R.; Morana, M.; Muhlbacher, D.; Scharber, M.; Brabec, C. J. *Macromolecules* **2007**, *40*, 1981–1986.
(28) Soci, C.; Hwang, I. W.; Moses, D.; Zhu, Z.; Waller, D.; Gaudiana, R.; Brabec, C. J.; Heeger, A. J. *Adv. Funct. Mater.* **2007**, *17*, 632–636.
(29) Lucas, L.; Mehdi, N. E.; Ho, H. A.; Belanger, D.; Breau, L. *Synthesis* **2000**, *9*, 1253–1258.
(30) Brzezinski, J. Z.; Reynolds, J. R. *Synthesis* **2002**, *8*, 1053–1056.
(31) Cossiella, R. F.; Akcelrud, L.; Atvars, D. Z. *J. Braz. Chem. Soc.* **2005**, *16*, 74–86.
(32) Chirvase, D.; Parisi, J.; Hummelen, J. C.; Dyakonov, V. *Nanotechnology* **2004**, *15*, 1317–1323.
(33) Li, G.; Yao, Y.; Hoichang, Y.; Shrotriya, V.; Guanwen, Y.; Yang, Y. *Adv. Funct. Mater.* **2007**, *17*, 1636–1644.
(34) Padinger, F.; Rittberger, R. S.; Sariciftci, N. S. *Adv. Funct. Mater.* **2003**, *13*, 85–55.

MA801945H